

Low-Intensity Light Therapy (1068 nm) Protects CAD Neuroblastoma Cells from β -Amyloid-Mediated Cell Death

Natalie A. Duggett and Paul L. Chazot*

School of Biological & Biomedical Sciences, Durham University, South Road, Durham, DH1 3LE, United Kingdom

*Corresponding author: Paul L. Chazot, School of Biological & Biomedical Sciences, Durham University, South Road, Durham, DH1 3LE, United Kingdom, Tel: +441913341305; E-mail: paul.chazot@durham.ac.uk

Received date: July 14, 2014; Accepted date: August 23, 2014; Published date: August 30, 2014

Copyright: © 2014 Duggett NA, et al. This is an open-access article distributed under the terms of the Creative Commons Attribution License, which permits unrestricted use, distribution, and reproduction in any medium, provided the original author and source are credited.

Abstract

Using a simple *in vitro* amyloidopathy CAD neuronal model, infrared (IR) 1068 nm light treatment (5 x 3 minutes) was investigated as a novel neuroprotection strategy. Synthetic human β -amyloid₍₁₋₄₂₎ peptide was subjected to aggregation in a test-tube, and shown to form fibrils of a range of sizes (individually ~10 μ m), which compromised the cellular nuclear integrity of CAD cells in culture, and elicited a dose-dependent neurotoxicity (β -amyloid₍₁₋₄₂₎ peptide concentration range 0-25 μ M) up to 73%, which was significantly suppressed (up to 24%; $p < 0.001$) by prior treatment with IR1068.

Keywords Photobiomodulation; Low Intensity Light Therapy; Near Infrared; β -amyloid

Abbreviations

A β , β -amyloid; AD, Alzheimer's disease; ATP, adenosine triphosphate; CAD, Cath.a differentiated; iNOS, inducible nitric oxide synthase; IR, infrared; IR1068, infrared at 1068 nm; LDH, lactate dehydrogenase; LILT, Low-Intensity Light Therapy; MMP+, 1-methyl-4-phenylpyridium; NIR, near-infrared; SP, senile plaque; UVA, ultra violet A.

Introduction

Infrared radiation (700-4000nm) has been reported to account for up to 40% of the solar radiation which reaches the earth's surface [1], Near Infrared (NIR) light, typically defined as 600-1500 nm, has been shown to have a wide range of biological actions and therapeutic benefits, and a great deal of research has been undertaken to establish the optimal parameters; whether they be wavelength, fluence, dosage or light source (Laser or LEDs) [2,3]. Low-Intensity Light Therapy (LILT), also known as photobiomodulation, has been reported to modulate a considerable number of biological processes in a significant number of studies. These include increasing wound healing rates [4-7]; induction of cellular proliferation in multiple cell culture systems; including osteoblasts [8-10], fibroblasts [11-13], muscle cells and epithelial cells [14,15]; improving the healing time of *Herpes labialis* infections [16]; increasing ATP synthesis and mitochondrial respiration rates [17-21].

LILT has also been shown to promote cell survival and protect against a number of insults *in vitro*, including UVA [22], potassium cyanide [23], methanol-derived format [24], MPP⁺ (1-methyl-4-phenylpyridium) and rotenone [25]. Neuronal culture provides a unique method to study every facet of neural processing with high reproducibility, in albeit a simplified system. The CAD (Cath.a-differentiated) cell lines are catecholaminergic cells, derived from the Cath.a cell line which was procured from a brain tumor that had developed in a transgenic mouse model. CAD cells spontaneously lost

their original oncogene after committing to a neuronal phenotype. The cell line expresses neurotransmitters, ion channels and neuron-specific proteins including active tyrosine hydroxylase and synaptophysin, all of which provide vital characteristics for the study of neuronal systems *in vitro* [26,27].

Alzheimer's disease is the leading cause of dementia in the world, it is a progressive dementia characterized by the deposition of β -amyloid (A β), found in large extracellular structures known as senile plaques (SPs), which are thought to induce toxicity through affecting the stability of the cell membrane therefore reducing synaptic transmission [28] and impairing synaptic plasticity [29]. Recent reports have suggested that A β oligomers, rather than insoluble fibrils, are the more toxic structure and there is only a weak correlation between quantity of plaques and neuronal loss [30-33]. Both structures have been found to be toxic *in vitro* with differential effects on neuronal viability, with oligomers as the more toxic species and plaques acting as A β reservoirs which can be utilised by oligomers [32-35]. The aim of this investigation was to produce an Alzheimer's disease model system *in vitro* with a range of A β structures. This model was designed to provide a heterogenous A β -species system, more realistic to the clinical situation than some methods currently in use. This model was adopted to study A β toxicity on a neuronal cell line and whether irradiation with IR1068 affected the level of this toxicity.

The strong absorption of NIR at long wavelengths by water generally limits the penetration of light into deep tissue. NIR at 1068 nm represents a peak in transmission through the water molecule and therefore requires less energy to safely enter biological materials, reducing thermal stress attributed to wavelengths 1300 nm and beyond [2,22].

The present study aimed also to investigate whether IR1068 causes proliferation as a secondary mechanism and whether treatment with IR1068 is able to protect against A β insults.

Materials and Methods

Cell maintenance

CAD (Cath.a – differentiated) Cells were maintained in Gibco® DMEM/F12 + GlutaMAX® and 10% foetal calf serum (FCS) in 75 cm² flasks until reaching 75% confluence, 3000 cells/mm². At this point they were passaged into 24 well plates, 450 μ l per well.

Preparation of β -amyloid fibrils for use in Neuronal Cultures

Human β -amyloid₍₁₋₄₂₎ peptide was purchased from Ascent Scientific, UK; upon arrival peptide was dissolved in DMSO to 1 mg/ml and stored at -80°C until use. Prior to use, the peptide was diluted to 200 μ M using sterile PBS. The peptide was then incubated for 72 hours at 37°C, 5% CO₂, without agitation. The peptide was then diluted to the required concentration using DMEM/F12 plus GlutaMAX® +10% FCS, inverted and gently added to neuronal cultures. Control cultures were conducted using the same DMSO: PBS ratio as for A β conditions, in DMEM/F12 plus GlutaMAX® +10% FCS.

Electron microscopy

Electron micrographs were obtained (Figure 1) to determine the structure of the β -amyloid peptide following fibril formation as described above. A sample of 200 μ M β -amyloid₍₁₋₄₂₎ peptide was imaged, prior to the use of the peptide in neuronal cultures. Samples were negative stained with 2% uranyl acetate, in distilled water, onto 400 mesh formvar coated copper grids and air dried. Samples were viewed using a Hitachi H7600 Transmission Electron Microscope. Dr Christine Richardson conducted all electron microscopy in the Histology laboratory within the University of Durham Imaging facility.

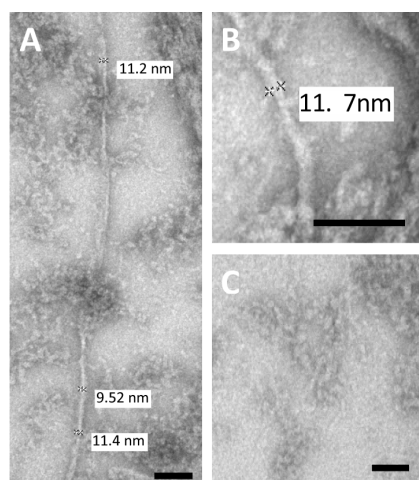


Figure 1: Representative electron micrograph of β -amyloid₍₁₋₄₂₎ fibrils/oligomers. Panels a and b show examples of fibrils, whereas c demonstrates amorphous oligomeric structures, formed by the method stated. Scale bar 100 nm.

Experimental Set-Up

CADs and A β

24 hours after cells were passed into 24 well plates they were exposed to five sets of 3 minute IR1068 \pm 10 or Sham treatments, 30 minutes apart, and cells were returned to the incubator. 24 hours after this time, media was removed and replaced with DMEM/F12 +GlutaMAX® +10% FCS containing the desired concentration of β -amyloid₍₁₋₄₂₎ peptide. Immediately after, cells were exposed to a second set of five 3 minute IR1068 or Sham exposures and returned to the incubator. 24 hours after the addition of β -amyloid₍₁₋₄₂₎, the cells were again exposed to five sets of 3 minute IR1068 or Sham treatments and again returned to the incubator. 24 hours after the third set of IR1068 or Sham exposures a CytoTox 96 Non-radioactive assay was performed on the cells.

Immunocytofluorescence with Ki67

CAD cells were passed into 24 well plates containing 13mm glass cover slipped and coated with poly-d lysine. Cells were maintained for 72 hours in DMEM/F12 +GlutaMAX® +10% FCS. After this time the media was changed and cells were exposed to five sets of three minute IR1068 or sham exposures with 30 minutes between each treatment. Following the final treatment, cultures were returned to the incubator for four hours. After this time, the media was removed from the wells and coverslips washed with PBS-T (PBS with 0.05% Tween-20) twice for five minutes each. Cells were fixed in 4% paraformaldehyde for 15 minutes and then washed twice, as stated previously. Cultures were then permeabilised using 0.5% Triton X-100 in PBS for 10 minutes and washed once more. PBG (1% BSA (Fraction V, minimum 96% lyophilized powder), 0.5% cold water fish skin gelatin in PBS, pH7.4) was used to block the cells for 15 minutes, after which the primary antibody was diluted in PBG; 1:400 anti-Ki67, and incubated with the primary antibody for one hour at room temperature. Cells were then washed three times using PBS-T and then incubated with the secondary antibodies (1:100 anti-DAPI (4',6-diamidino-2-phenylindole) & 1:500 anti-rabbit Alexa fluor 488) for one hour. Following five washes with PBS-T, coverslips were mounted onto glass slides with Mowiol (Calbiochem, UK) and left to dry overnight at room temperature in the dark, before storage at 4°C. Cells were inspected using a Carl Zeiss Axioskop 2 microscope equipped for epifluorescence. Images were captured using a Hamamatsu Orca 285 CCD camera controlled by Improvision Volocity software version 6.

CytoTox 96 non-radioactive assay (Promega, UK)

CytoTox 96 assay kit quantifies LDH (lactate dehydrogenase) levels as a measure of cell lysis (necrosis). Media was removed from cells and centrifuged at 13,000 rpm for two minutes. The supernatant containing the LDH was retained and the pellet re suspended in PBS, using the same volume removed from the cells, and placed back into each well of the 24 well plates. The 24 well plates were then frozen for two hours at -20°C to lyse all remaining cells. Cells were subsequently thawed and centrifuged at 13,000 rpm for two minutes; again the supernatant was retained as a measure of total LDH. Dilutions; 1:10 and 1:20, were made of each supernatant using PBS as the diluent with DMEM+F12 plus 10% FCS to calibrate the assay. Neat, 1:10 and 1:20 dilutions were all completed in triplicate. 50 μ l of substrate mix was added to 50 μ l of each dilution prior to incubation for 30 minutes at room temperature in the dark. Following this, 50 μ l of stop solution

was added to each dilution and the absorbance measured at 490 nm on a Mullikan Ascent Plate Reader, Version 2.6. LDH release was normalized against the sum of total LDH absorbance, combining the absorbance of positive control freeze-thawed cells and absorbance of initial media containing LDH readings.

Statistics

Data were analysed using a Student's two tailed T-test for immunofluorescence analysis. Data were analysed using a 2-way ANOVA analysis of variance, using a Bonferroni post-test. Data are mean \pm SEM, with a confidence interval of 95%. All analyses were conducted using GraphPad Prism Version 5.0.

LED Arrays

1068 nm emitting LED arrays have a bandwidth of approximately 25nm, pulsed at 600 Hz, with a duty cycle of 300 microseconds, 5mW/cm². Sham treatments were conducted using the same array but with aluminium foil placed over the cells. LED arrays were supplied by Virulite Distribution Ltd, UK and were validated by both Dr Gordon Dougal (Virulite Distribution Ltd, UK) and the Durham Physics Department (Dr Andrew Beeby).

Results

Amyloid appearance

Following staining of A β 42 peptide, fibrils/oligomers were imaged. Structures that had formed were heterogenous; there were large β -pleated sheet structures, which spanned moderate areas of the formvar grids. These sheet-like structures appeared to be comprised of multiple smaller long fibrillar structures, which were measured to be approximately 10 nm, as shown in figure 1. These appeared throughout the samples and often appeared directly adjacent to large β -pleated sheets, however it is unclear whether these structures merged to form the beta-pleated sheet or whether the fibrils were products of the large sheet of peptide.

CAD Cells, A β - induced toxicity and IR1068 protection

Exposure to IR1068 had no significant effect compared to sham treated controls against cell death when cells were exposed to PBS, 0.5 μ M or 1 μ M A β ₄₂. However, there was a trend for a reduction in cell death in the IR1068 treated condition, compared to sham treated controls (n= 6, p <0.1) at 2.5 μ M A β .

At 3.5 μ M A β , treatment of CAD cells with IR1068 elicited a statistically significant reduction in cell death (n= 6, p <0.05), and this was increased at 4.5 μ M A β (n= 6, p <0.01) and 5 μ M A β (n=6, p <0.01) compared to sham treated controls.

Concentrations of A β at 10 μ M and 25 μ M were exceedingly toxic to Sham treated cells, causing approximately 58% and 73% cell death, respectively. However, despite the high concentrations of A β treated of cells with IR1068 significantly reduced cell death to 44% and 60%, respectively (n= 6, p <0.001, both concentrations).

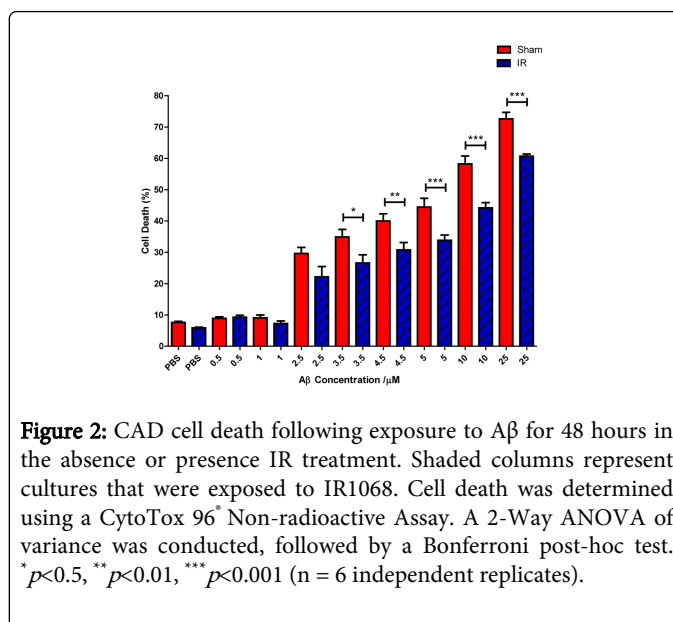
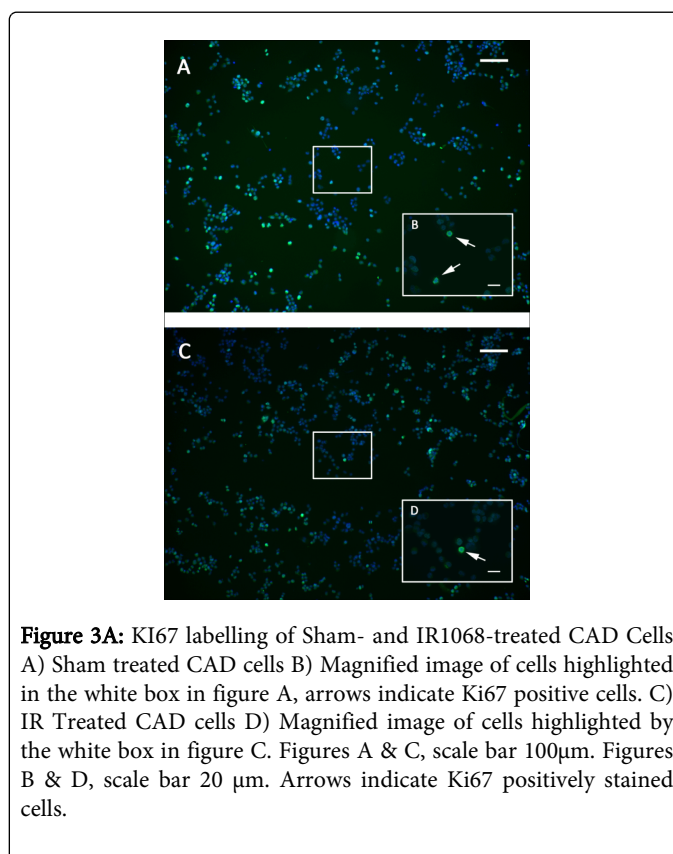


Figure 2: CAD cell death following exposure to A β for 48 hours in the absence or presence IR treatment. Shaded columns represent cultures that were exposed to IR1068. Cell death was determined using a CytoTox 96[®] Non-radioactive Assay. A 2-Way ANOVA of variance was conducted, followed by a Bonferroni post-hoc test. * p <0.05, ** p <0.01, *** p <0.001 (n = 6 independent replicates).

IR1068 and proliferation assessment in CAD cells

Ki67 positive cells are a marker of cellular proliferation. IR1068-treated neuronal cultures displayed no significant difference in the proportional of cells that stained positive for Ki67 when compared to sham-treated neuronal cultures (p = 0.83). Figure 3A shows illustrative immune cytofluorescence images of sham and IR1068 treated CAD cells and figure 3B shows statistical analysis of staining quantification.



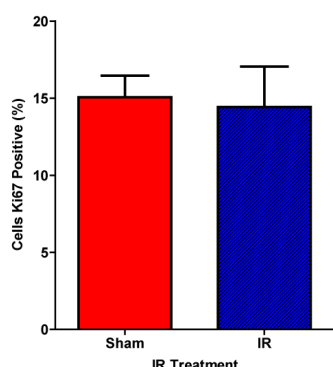


Figure 3B: Effect of IR1068 on proliferation. IR1068 exposure has no apparent significant effect on cell proliferation, compared to sham-treated cell cultures; Ki67 was used as a proliferation marker. Values are given as a percentage of the total number of cells counted. Data shown mean value \pm SEM, n=6 replicate individual cultures.

Discussion

There are a significant number of techniques which are in use to form $A\beta$ plaques from synthetic $A\beta$ peptide. The advantage of 'growing' $A\beta$ structures in vitro lies in the fact that conditions can be tightly controlled and manipulated to create a particular structure or a mixture of structures. However, there is not a 'standard' method for the formation of $A\beta$ oligomers or aggregates; this has resulted in the ability of structures formed in different conditions to have significantly different efficacies despite being formed from the same starting peptide [30,31]. A number of methods are used for the creation of toxic $A\beta$ structures from synthetic peptides, with a wide range of permutations exacted to push structure formation towards fibrils or oligomers [35-41]. An aim for this investigation was to create an Alzheimer's disease model system in vitro, and to create a relatively simple method through which a range of $A\beta$ -derived structures could be formed, which perhaps more closely represent what is present clinically present in the Alzheimer's disease brain than other techniques published [33,35,37,38]. Fibrils formed through the method described herein, were approximately 10 nm in diameter with diffuse oligomeric-type structures forming alongside fibrils. In concentrated solutions, fibrils were present as large pleated-sheet structures, with individual fibrils observable in the sheets and appearing to be joining or leaving the structures. Amorphous oligomers were observable throughout the solution, often concentrated around branches of the fibrillar structures (Shown in figure 1, the same range as diameters previously reported in vitro [34,37].

A secondary aim was to investigate whether this synthetic $A\beta$ had any effect on cell death, and if IR1068 exposure altered the degree of $A\beta$ -induced cell toxicity. $A\beta$ deposition was clearly visible, adjacent to damaged CAD cells with nuclei of a granular appearance. IR1068 exposure was found to consistently significantly reduce cell death caused by $A\beta$, by up to 24%, over the range of $A\beta$ concentrations (1-25 μ M). The range of $A\beta$ concentrations used would not necessarily be found in vivo. However, the use of potentially unrealistic

concentrations in vitro is a necessary experimental limitation, as synthetic $A\beta$ peptides have been reported to be less neurotoxic than cell-derived $A\beta$ [32]. However, there is evidence to suggest cellular concentrations of $A\beta$ can reach micromolar levels in vesicular compartments, so concentrations used in this investigation have relevance [42].

LILT at various wavelengths has been previously shown to induce proliferation in various cell types. As 1068 nm is in the middle of the 'optical window' of NIR, with little absorption by the water molecule or major tissue chromophores, such as haemoglobin or melanin, it requires less energy to penetrate biological matter and thus there is less risk of thermal stress and tissue damage [2,3]. This investigation provided preliminary evidence that IR1068 has no effect on cellular proliferation in the CAD cell line and that active proliferation is unlikely to be the cause of the apparent reduced cell death/improved viability that has been observed following IR1068 exposure.

These data further support beneficial effects reported by our group following LILT at 1068 nm, including improved working memory in ageing mice [43], reduction of $A\beta$ levels in an AD mouse model [44], protection of primary cortical neurons from glutamate-induced cytotoxicity (unpublished data), enhanced cell viability following UVA insult [22] and improved healing time associated with herpes labialis infections [16]. The mechanism through which IR1068 elicits its biological effects remains unclear. However, IR1068 has been shown to upregulate iNOS (inducible nitric oxide synthase) levels in conjunction with reduced apoptosis [22], with NO believed to act in the prevention of caspase-3 activation [45-47], however this has not been shown to prevent apoptosis in neuronal cell types [48]. Work recently published in our laboratory [44] and on-going investigations have consistently recorded up regulation of a number of heat shock proteins (HSP) proteins including HSP105, HSP70, and HSP27 in a number of mouse strains following exposure to IR1068. The reduction in cell death reported here could be attributed to the up regulation of these chaperones due to the significant number of roles in maintenance of homeostasis; including preventing cell death through both the intrinsic and extrinsic apoptosis pathways [49-52], as well as reducing cellular stress through direction of aggregates towards ubiquitin/proteasome machinery [49,53-55] or via direct refolding [56-59], and have been reported to comprise up to 5% of the cellular proteins [60]. Profound up regulation of HSPs persistently recorded in mammalian tissue following IR1068 exposure may be due to a process called 'thermal relaxation'. A small amount of local thermal energy may be emitted from the photo acceptors upon absorption of NIR. This transient local energy (not affecting the entire cell) has been shown to alter local biochemical activity, which could give rise to secondary signalling processes which ultimately result in neuroprotection in the face of insults [19, 61]. The induction of these mechanisms, or a combination of these mechanisms, following IR1068 exposure are sufficient to explain the reduced cell death reported in cultures exposed to IR1068, independent of proliferation.

Important investigations are underway in the laboratory to characterize the panel of heat shock proteins expressed in the CAD cell line as functionality differs significantly across the chaperone family. 1068 nm is not the first wavelength of NIR shown to be neuroprotective, studies conducted at 633 nm [62], 670 nm [23,25,63-65] and 830 nm [64] have all also proved to be neuroprotective against a variety of insults. The results of this investigation demonstrate that infrared light at the far end of the NIR spectrum, IR1068, is able to protect against cell death following a series

of exposures in a neuronal cell line, in the presence of the aggregate believed to be a principal contributor to Alzheimer's disease. This study has provided a model system in which to further study the pathogenic effects of $A\beta$ and protective attributes of IR1068 in a neuronal cell line.

The use of IR1068 as a treatment for Alzheimer's disease is under investigation, with recruitment of patients initiated in December 2010 (double-blind, placebo-controlled clinical trial). The results of these trials will enable statistically valid conclusions to be drawn, regarding the use of IR1068 as a treatment for neurodegenerative disease in a clinical setting. Preliminary results from this investigation demonstrate protective effects for IR1068 however significant work remains to be conducted by the neuroscience community to model the complex nature of Alzheimer's disease accurately in vitro.

Acknowledgements

Thanks go to Dr Christine Richardson of the Electron Microscopy Unit at Durham University for assistance with imaging. This study was supported by the BBSRC (UK) and Durham University Biophysical Sciences Institute; the sponsors had no role in the research, preparation of the manuscript or decision to publish.

References

1. Frank S, Oliver L, Lebreton DE, Coster C, Moreau C, et al. (2004) Infrared radiation affects the mitochondrial pathway of apoptosis in human fibroblasts. *J Invest Dermatol* 123: 823-31.
2. Tsai CL, Chen JC, Wang WJ (2001) Near-Infrared Absorption Property of Biological Soft Tissue Constituents. *Journal of Medical and Biological Engineering* 21:7-14.
3. Hamblin MR., Demidova TN (2006) Mechanisms of low level light therapy. *Proc. of SPIE* 6140: 614001-614012.
4. Mester E, Spiry T, Szende B, Tota JG (1971) Effect of laser rays on wound healing. *Am J Surg* 122: 532-535.
5. Chung TY, Peplow PV, Baxter GD (2010) Laser photobiomodulation of wound healing in diabetic and non-diabetic mice: effects in splinted and unsplinted wounds. *Photomed Laser Surg* 28:251-61.
6. Marchionni AM, Medrado AP, Silva TM, Fracassi LD, Pinheiro AL, et al. (2010) Influence of laser (λ 670 nm) and dexamethasone on the chronology of cutaneous repair. *Photomed Laser Surg* 28: 639-46.
7. Santos NR, Dos Santos JN, Sobrinho JB, Ramalho LM and Carvalho CM, et al. (2010) Effects of laser photobiomodulation on cutaneous wounds treated with mitomycin C: a histomorphometric and histological study in a rodent model. *Photomed Laser Surg* 28: 81-90.
8. Ueda Y, Shimizu N (2003) Effects of pulse frequency of low-level laser therapy (LLLT) on bone nodule formation in rat calvarial cells. *J Clin Laser Med Surg* 21: 271-217.
9. Pires Oliveira DA, De Oliveira RF, Zangaro RA, Soares CP (2008) Evaluation of low-level laser therapy of osteoblastic cells. *Photomed Laser Surg* 26: 401-404.
10. Kreisler M., Christoffers AB, Willershausen B, DHOedt B (2003) Effect of low-level GaAlAs laser irradiation on the proliferation rate of human periodontal ligament fibroblasts: an in vitro study. *J Clin Periodontol* 30: 353-358.
11. Vinck EM, Cagnie BJ, Cornelissen MJ, Declercq HA, Cambier DC (2003) Increased fibroblast proliferation induced by light emitting diode and low power laser irradiation. *Lasers Med Sci* 18: 95-99.
12. Hawkins DH, Abrahamse H (2006) The role of laser fluence in cell viability, proliferation, and membrane integrity of wounded human skin fibroblasts following helium-neon laser irradiation. *Lasers Surg Med* 38: 74-83.
13. Taniguchi D, Dai P, Hojo T, Yamaoka Y, Kubo T, et al. (2009) Low-energy laser irradiation promotes synovial fibroblast proliferation by modulating p15 subcellular localization. *Lasers Surg Med* 41: 232-239.
14. Whelan HT, Smits RL, Buchman JR, Whelan EV, Turner NT, et al. (2001) Effect of NASA light-emitting diode irradiation on wound healing. *J Clin Laser Med Surg* 19, 305-314.
15. Sommer AP, Pinheiro AL, Mester AR, Franke RP, Whelan HT (2001) Bistimulatory windows in low-intensity laser activation: lasers, scanners, and NASA's light-emitting diode array system. *J Clin Laser Med Surg* 19: 29-33.
16. Dougal G, Kelly P (2001) A pilot study of treatment of herpes labialis with 1068 nm narrow waveband light. *Clin Exp Dermatol* 26: 149-154.
17. Passarella S, Casamassima E, Molinari S, Pastore D and Quagliariello E, et al. (1984). Increase of proton electrochemical potential and ATP synthesis in rat liver mitochondria irradiated in vitro by helium-neon laser. *FEBS Lett* 175: 95-99.
18. Wilden L, Karthein R (1998) Import of radiation phenomena of electrons and therapeutic low-level laser in regard to the mitochondrial energy transfer. *J Clin Laser Med Surg* 16: 159-165.
19. Karu T, Tiphlova O, Esenaliev R, Letokhov V (1994) Two different mechanisms of low-intensity laser photobiological effects on *Escherichia coli*. *J Photochem Photobiol B* 24: 155-161.
20. Chen AC, Arany PR, Huang YY, Tomkinson EM and Sharma SK et al. (2011). Low-level laser therapy activates NF- κ B via generation of reactive oxygen species in mouse embryonic fibroblasts. *PLoS One* 6: e22453.
21. Mochizuki ON, Kataoka Y, Cui Y, Yamada H, Heya M, et al. (2002) Effects of near-infra-red laser irradiation on adenosine triphosphate and adenosine diphosphate contents of rat brain tissue. *Neurosci Lett* 323, 207-210.
22. Bradford A, Barlow A, Chazot PL (2005) Probing the differential effects of infrared light sources IR1072 and IR880 on human lymphocytes: evidence of selective cytoprotection by IR1068. *J Photochem Photobiol B* 81: 9-14.
23. Liang HL, Whelan HT, Eells JT, Meng H, Buchmann E, et al. (2006) Photobiomodulation partially rescues visual cortical neurons from cyanide-induced apoptosis. *Neuroscience* 139: 639-649.
24. Eells JT, Henry MM, Summerfelt P, Wong-Riley MT and Buchmann EV, et al. (2003) Therapeutic photobiomodulation for methanol-induced retinal toxicity. *Proc Natl Acad Sci U S A* 100: 3439-3444.
25. Liang H, Whelan HT, Eells JT, Wong-Riley MT (2008) Near-infrared light via light-emitting diode treatment is therapeutic against rotenone- and 1-methyl-4-phenylpyridinium ion-induced neurotoxicity. *Neuroscience* 153: 963-974.
26. Qi Y, Wang JK, Mcmillian M, Chikaraishi DM (1997) Characterization of a CNS cell line, CAD, in which morphological differentiation is initiated by serum deprivation. *J Neurosci* 17: 1217-1225.
27. Scholzen T, Gerdes J (2000) The Ki-67 protein: from the known and the unknown. *J Cell Physiol* 182: 311-322.
28. Kamenetz F, Tomita T, Hsieh H, Seabrook G, and Borchelt D, et al. (2003) APP processing and synaptic function. *Neuron* 37, 925-937.
29. Shankar GM, Li S, Mehta TH, Garcia-Munoz A and Shepardson NE, et al. (2008). Amyloid-beta protein dimers isolated directly from Alzheimer's brains impair synaptic plasticity and memory. *Nat Med* 14: 837-842.
30. Benilova I, Karran E, De Strooper B (2012) The toxic A β oligomer and Alzheimer's disease: an emperor in need of clothes. *Nat Neurosci* 15, 349-357.
31. Haass C, Selkoe DJ (2007) Soluble protein oligomers in neurodegeneration: lessons from the Alzheimer's amyloid beta-peptide. *Nat Rev Mol Cell Biol* 8: 101-112.
32. Dahlgren KN, Manelli AM, Stine WB, Baker LK., Krafft GA, Ladu MJ (2002) Oligomeric and fibrillar species of amyloid-beta peptides differentially affect neuronal viability. *J Biol Chem* 277: 32046-32053.

33. Sondag CM, Dhawan G, Combs CK (2009) Beta amyloid oligomers and fibrils stimulate differential activation of primary microglia. See comment in PubMed Commons below J Neuroinflammation 6: 1.
34. Hartley DM, Walsh DM, Ye CP, Diehl T and Vasquez S, et al. (1999) Protofibrillar intermediates of amyloid beta-protein induce acute electrophysiological changes and progressive neurotoxicity in cortical neurons. J Neurosci 19: 8876-8884.
35. Kaye R, Head E, Thompson JL, McIntire TM, Milton SC, et al. (2003) Common structure of soluble amyloid oligomers implies common mechanism of pathogenesis. Science 300: 486-489.
36. Kranenburg O, Bouma B, Gent YY, Aarsman CJ and Kaye R, et al. (2005). Beta-amyloid (A β) causes detachment of N1E-115 neuroblastoma cells by acting as a scaffold for cell-associated plasminogen activation. Mol Cell Neurosci 28: 496-508.
37. Lorenzo A, Yankner BA (1994) Beta-amyloid neurotoxicity requires fibril formation and is inhibited by Congo red. See comment in PubMed Commons below Proc Natl Acad Sci U S A 91: 12243-12247.
38. Isobe I, Yanagisawa K, Michikawa M (2000) A possible model of senile plaques using synthetic amyloid beta-protein and rat glial culture. See comment in PubMed Commons below Exp Neurol 162: 51-60.
39. Kudva YC, Hiddinga HJ, Butler PC, Mueske CS, Eberhardt NL (1997) Small heat shock proteins inhibit in vitro A β (1-42) amyloidogenesis. See comment in PubMed Commons below FEBS Lett 416: 117-121.
40. King M, Nafar F, Clarke J, Mearow K (2009) The small heat shock protein Hsp27 protects cortical neurons against the toxic effects of beta-amyloid peptide. See comment in PubMed Commons below J Neurosci Res 87: 3161-3175.
41. El-Agnaf OM, Nagala S, Patel BP, Austen BM (2001) Non-fibrillar oligomeric species of the amyloid A β peptide, implicated in familial British dementia, are more potent at inducing apoptotic cell death than protofibrils or mature fibrils. See comment in PubMed Commons below J Mol Biol 310: 157-168.
42. Hu X, Crick SL, Bu G, Frieden C, Pappu RV, et al. (2009) Amyloid seeds formed by cellular uptake, concentration, and aggregation of the amyloid-beta peptide. See comment in PubMed Commons below Proc Natl Acad Sci U S A 106: 20324-20329.
43. Michalikova S, Ennaceur A, van Rensburg R, Chazot PL (2008) Emotional responses and memory performance of middle-aged CD1 mice in a 3D maze: effects of low infrared light. See comment in PubMed Commons below Neurobiol Learn Mem 89: 480-488.
44. Grillo SL, Duggett NA, Ennaceur A, Chazot PL (2013) Non-invasive infra-red therapy (1072 nm) reduces I β -amyloid protein levels in the brain of an Alzheimer's disease mouse model, TASTPM. See comment in PubMed Commons below J Photochem Photobiol B 123: 13-22.
45. Rössig L, Fichtlscherer B, Breitschopf K, Haendeler J, Zeiher AM, et al. (1999) Nitric oxide inhibits caspase-3 by S-nitrosation in vivo. See comment in PubMed Commons below J Biol Chem 274: 6823-6826.
46. Marrot L, Belaïdi JP, Lejeune F, Meunier JR, Asselineau D, et al. (2004) Photostability of sunscreen products influences the efficiency of protection with regard to UV-induced genotoxic or photoageing-related endpoints. See comment in PubMed Commons below Br J Dermatol 151: 1234-1244.
47. Kim YM, Talanian RV, Billiar TR (1997) Nitric oxide inhibits apoptosis by preventing increases in caspase-3-like activity via two distinct mechanisms. See comment in PubMed Commons below J Biol Chem 272: 31138-31148.
48. Zhou P, Qian L, Iadecola C (2005) Nitric oxide inhibits caspase activation and apoptotic morphology but does not rescue neuronal death. See comment in PubMed Commons below J Cereb Blood Flow Metab 25: 348-357.
49. Lanneau D, Wettstein G, Bonniaud P, Garrido C (2010) Heat shock proteins: cell protection through protein triage. See comment in PubMed Commons below ScientificWorldJournal 10: 1543-1552.
50. Beere HM (2004) "The stress of dying": the role of heat shock proteins in the regulation of apoptosis. See comment in PubMed Commons below J Cell Sci 117: 2641-2651.
51. Beere HM (2005) Death versus survival: functional interaction between the apoptotic and stress-inducible heat shock protein pathways. See comment in PubMed Commons below J Clin Invest 115: 2633-2639.
52. Yenari MA, Liu J, Zheng Z, Vexler ZS, Lee JE, et al. (2005) Antiapoptotic and anti-inflammatory mechanisms of heat-shock protein protection. See comment in PubMed Commons below Ann N Y Acad Sci 1053: 74-83.
53. Sahara N, Maeda S, Yoshiike Y, Mizoroki T, Yamashita S, et al. (2007) Molecular chaperone-mediated tau protein metabolism counteracts the formation of granular tau oligomers in human brain. See comment in PubMed Commons below J Neurosci Res 85: 3098-3108.
54. Muchowski PJ, Wacker JL (2005) Modulation of neurodegeneration by molecular chaperones. See comment in PubMed Commons below Nat Rev Neurosci 6: 11-22.
55. Rogalla T, Ehrnsperger M, Preville X, Kotlyarov A, Lutsch G, et al. (1999). Regulation of Hsp27 oligomerization, chaperone function, and protective activity against oxidative stress/tumor necrosis factor alpha by phosphorylation. J Biol Chem, 274: 18947-18956.
56. Söti C, Nagy E, Giricz Z, Vigh L, Csermely P, et al. (2005) Heat shock proteins as emerging therapeutic targets. See comment in PubMed Commons below Br J Pharmacol 146: 769-780.
57. Ecroyd H, Carver JA (2009) Crystallin proteins and amyloid fibrils. See comment in PubMed Commons below Cell Mol Life Sci 66: 62-81.
58. Calderwood SK, Murshid A, Prince T (2009) The shock of aging: molecular chaperones and the heat shock response in longevity and aging--a mini-review. See comment in PubMed Commons below Gerontology 55: 550-558.
59. Turturici G, Sconzo G, Geraci F (2011) Hsp70 and its molecular role in nervous system diseases. See comment in PubMed Commons below Biochem Res Int 2011: 618127.
60. Soti C, Csermely P (2003) Aging and molecular chaperones. See comment in PubMed Commons below Exp Gerontol 38: 1037-1040.
61. Karu T, Pyatibrat L, Kalendo G (1995) Irradiation with He-Ne laser increases ATP level in cells cultivated in vitro. See comment in PubMed Commons below J Photochem Photobiol B 27: 219-223.
62. Rojas JC, Lee J, John JM, Gonzalez-Lima F (2008) Neuroprotective effects of near-infrared light in an in vivo model of mitochondrial optic neuropathy. See comment in PubMed Commons below J Neurosci 28: 13511-13521.
63. Giuliani A, Lorenzini L, Gallamini M, Massella A, Giardino L, et al. (2009) Low infra red laser light irradiation on cultured neural cells: effects on mitochondria and cell viability after oxidative stress. See comment in PubMed Commons below BMC Complement Altern Med 9: 8.
64. Wong-Riley MT, Liang HL, Eells JT, Chance B, Henry MM, et al. (2005) Photobiomodulation directly benefits primary neurons functionally inactivated by toxins: role of cytochrome c oxidase. J Biol Chem, 280: 4761-4771.

This article was originally published in a special issue, entitled: "**Novel Treatment Strategies for Neurological and Neurodegenerative Diseases**", Edited by Simon Kaja, University of Missouri, USA